Ulvrova, M. M., Brune, S., Williams, S. (2019): Breakup without borders: how continents speed up and slow down during rifting. - *Geophysical Research Letters*, *46*, 3, pp. 1338—1347.

DOI: http://doi.org/10.1029/2018GL080387

Geophysical Research Letters

RESEARCH LETTER
10.1029/2018GL080387

Key Points:
- We investigate rift dynamics without imposed lateral boundaries using 2-D spherical annulus numerical models
- Continental rupture exhibits a multiphase evolution: (1) slow rifting, (2) sudden acceleration and breakup, (3) fast drifting, and (4) drift slow-down
- Abrupt plate speed-up during rifting generates enhanced convergence at existing plate boundaries or induces subduction initiation

Supporting Information:
- Supporting Information S1
- Movie S1
- Movie S2
- Movie S3
- Movie S4

Correspondence to:
M. M. Ulvrova,
martina.ulvrova@erdw.ethz.ch

Citation:
Ulvrova, M. M., Brune, S., & Williams, S. (2019). Breakup without borders: How continents speed up and slow down during rifting. *Geophysical Research Letters*, *46*, 1338–1347. https://doi.org/10.1029/2018GL080387

Received 6 SEP 2018
Accepted 19 DEC 2018
Accepted article online 26 DEC 2018
Published online 14 FEB 2019

Breakup Without Borders: How Continents Speed Up and Slow Down During Rifting

Martina M. Ulvrova[1], **Sascha Brune**[2,3], **and Simon Williams**[4]

[1]Institute of Geophysics, ETH Zürich, Zürich, Switzerland, [2]GFZ German Research Centre for Geosciences, Potsdam, Germany, [3]Institute of Earth and Environmental Science, University of Potsdam, Potsdam, Germany, [4]EarthByte Group, School of Geosciences, University of Sydney, Sydney, New South Wales, Australia

Abstract Relative plate motions during continental rifting result from the interplay of local with far-field forces. Here we study the dynamics of rifting and breakup using large-scale numerical simulations of mantle convection with self-consistent evolution of plate boundaries. We show that continental separation follows a characteristic evolution with four distinctive phases: (1) an initial slow rifting phase with low divergence velocities and maximum tensional stresses, (2) a synrift speed-up phase featuring an abrupt increase of extension rate with a simultaneous drop of tensional stress, (3) the breakup phase with inception of fast sea-floor spreading, and (4) a deceleration phase occurring in most but not all models where extensional velocities decrease. We find that the speed-up during rifting is compensated by subduction acceleration or subduction initiation even in distant localities. Our study illustrates new links between local rift dynamics, plate motions, and subduction kinematics during times of continental separation.

Plain Language Summary While the continents are spread out across the Earth at present day, we know that at various times in Earth's history these same continents were assembled together in larger "supercontinents". These supercontinents eventually fragment by a process called continental rifting, but certain aspects of the kinematic evolution of this process remained elusive so far. We created a series of sophisticated computer simulations of mantle convection in which continental rifts emerge naturally when the forces acting on assembled continents become large enough to break them apart. The simulations show that continental breakup involves a positive feedback loop, where the faster the continents move apart, the more quickly the connection between them weakens—similar to a rope that is stretched until it yields and eventually snaps. This speed-up of the continents can trigger the formation of new plate boundaries elsewhere on Earth, even at large distance to the rift. We also find that the continents often slow down again once the continents are separated and a new ocean basin is formed.

1. Introduction

Rifting of continents is an integral component of the Wilson cycle and a key ingredient in Earth's plate tectonic history, being the geodynamic process that forms new continental margins. Rift velocity is thought to be one of the key parameters controlling fault evolution and rift symmetry (Brune et al., 2014; Huismans & Beaumont, 2003; Tetreault & Buiter, 2018), while the rate of extension also governs melt production and affects the volcanic or magma-poor nature of rifted margins (Davis & Lavier, 2017; Lundin et al., 2018; Pérez-Gussinyé et al., 2006). Nevertheless, the geodynamic factors that control the evolution of rift velocity and strain localization from inception of rifting to breakup of continents and beyond are not understood in detail (Buck, 2015; Brune, 2016; Ziegler & Cloetingh, 2004).

Rift velocities for specific rifted margins can be estimated by combining full-fit plate reconstructions with available geological indicators such as synrift sedimentation, rift-related volcanism, seismic tectono-stratigraphy, and dated rocks from the continent-ocean transition (Buck, 2015). Many margins appear to involve a slow initial rift phase, followed by a characteristic increase of the rift velocity and finally a fast rift phase prior to continental separation (e.g., Heine et al., 2013; Kneller et al., 2012; McQuarrie & Wernicke, 2005). Concurrently, a characteristic rift velocity evolution can be inferred from analytical or numerical models of lithospheric extension, which reproduces the observed slow/fast velocity evolution and shows that the loss of rift strength is responsible for the abrupt rift acceleration (Brune et al., 2016).

Previous numerical rift models belong to one of two categories. Models with velocity boundary conditions usually impose constant velocities at the lateral model sides, which allows to study the effect of extension rate on rift processes (e.g., Ammann et al., 2017; Armitage et al., 2018; Brune et al., 2017). More complex setups involve temporarily varying velocities to match observations (e.g., Koptev et al., 2015; Naliboff & Buiter, 2015; Salerno et al., 2016) or spatially varying velocities mimicking basin opening around an Euler pole (Mondy et al., 2017). All of these models, however, have the disadvantage that rift velocities have to be known a priori. A second category of models apply a constant extensional force in order to investigate how rift velocities evolve through time (Brune et al., 2012, 2013; Takeshita & Yamaji, 1990). These models nonetheless suffer from the limitation that the force applied at the model boundaries is uniform through time. Another problem of rift models with force boundary conditions is that the necking instability, that is, the rift localization during thinning of the lithosphere, leads to exponentially growing rift velocities (Takeshita & Yamaji, 1990), such that the bulk extension rates eventually reach unrealistically high values unless a switch to velocity boundary conditions at a limiting velocity is implemented (Heine & Brune, 2014).

The problem of reproducing rift velocity evolution in models with imposed lateral boundary conditions is linked to the simple fact that there are no lateral boundaries in nature. Instead, the plate tectonic driving forces slab pull, basal drag, and ridge push (Forsyth & Uyeda, 1975), which ultimately derive from buoyancy variations in Earth's interior, interact with local rift forces such as rift strength, topography-induced tension, and thermal buoyancy (Brune, 2018) in a self-consistent manner that can neither be fully described through velocity nor force boundary conditions.

In this study, we investigate the prerift, synrift, and postrift dynamics of continental extension using 2-D spherical annulus models of mantle convection with continents. Similar models have been previously used to study supercontinent cyclicity statistically (Rolf et al., 2014), but here we focus on the dynamics of rifting. In contrast to previous regional rift models, our simulations avoid the necessity to impose lateral boundary conditions so that rifting develops self-consistently as a response to the overall dynamics of the system. After introducing the model setup, we describe 10 different model scenarios and compare their velocity evolutions to plate tectonic reconstructions of key natural examples. In doing so we propose four characteristic phases to describe extensional evolution and suggest potential causes for each phase.

2. Model Setup

To capture the dynamics of the Earth's interior and its surface expression, we solve for the equations of conservation of mass, momentum, and energy and for the advection of different material compositions. Temperature, pressure, velocity flow, and composition solutions are found in dimensionless space and have to be scaled in order to be compared to Earth dynamics (for nondimensional equations and governing parameters, description of the initial conditions, and scaling procedure, see supporting information; Coltice et al., 2012; Müller et al., 2016; Turcotte & Schubert, 2002).

In our model, the mantle is heated from the core and from within. The internal heating rate is set to $H = 20$ that corresponds to 2.77×10^{-11} W/kg. This value of H results in a system that is controlled by the dynamics of the top boundary layer while the core contributes about 20% to the total surface heat budget, which falls into the estimated interval for the Earth of 10–40% (Jaupart et al., 2015). Both the top and the bottom boundaries are kept isothermal and free slip so that we neglect vertical deformation of the surface and development of topography. Compared to regional rift models, our setup does not require any lateral boundary conditions. This advantage is balanced by lower resolution compared to lithospheric-scale models.

Viscosity η is strongly temperature dependent and follows the Arrhenius law:

$$\eta(T,p) = \eta_A \exp\left(\frac{E_a + p\,V_a}{RT}\right), \tag{1}$$

with $V_a = 6.34 \cdot 10^{-7}$ m^3/mol the activation volume and $E_a = 170$ kJ/mol the activation energy. R is the gas constant, T the absolute dimensional temperature, and p the pressure. η_A is set such that η matches the reference viscosity η_0 at temperature 1,600 K and at zero pressure. We apply a viscosity cutoff at $10^4\,\eta_0$ to limit the viscosity variations to 6 orders of magnitude over ΔT, the temperature drop over the mantle.

In order to localize strain and obtain a plate-like surface, we adopt pseudo-plastic yielding (Moresi & Solomatov, 1998; Tackley, 2000a; 2000b). Rocks are softened and viscosity decreases with increasing strain rate $\dot{\epsilon}$ beyond a certain stress threshold, the yield stress σ_Y according to $\eta_Y = \sigma_Y/(2\dot{\epsilon})$. σ_Y is parameterized via a surface yield stress and a yield gradient that describes a linearly increasing yield stress with depth. Yielding parameters are listed in Table S1 together with physical parameters of the model given in Table S2.

We also prescribe weak oceanic crust that decouples to a certain degree the sinking slab from the overriding plate causing subduction asymmetry (Crameri et al., 2012; Gerya et al., 2008; Tagawa et al., 2007). The crust is neutrally buoyant, and it follows the same viscosity law as ambient mantle while being 10 times less viscous and more easily deformable. The thickness of the crust is 20 km so that it can be resolved numerically (having at least two 10-km-thick grid cells within the crustal material). It is formed at the ridges, dives back to the mantle at the trenches, and after reaching 290-km depth is converted to regular mantle material. Using such rheology results in self-consistent formation of strong plate interiors moving with a constant velocity delimited by narrow plate boundaries with reduced viscosity. Importantly, such rheology is sufficiently realistic to investigate global surface tectonics (Coltice et al., 2017).

Continental rafts are modeled using tracers (Rolf & Tackley, 2011; Rolf et al., 2017; Tackley & King, 2003). We consider two continents of identical shape with interiors that are 300 km thick and 3,600 km wide surrounded by 140-km-thick belts following the thickness of Archean cratons and Proterozoic belts. The width of the belts is 1,200 km. At each time step, continents cover in total 30% of the model surface. To ensure the stability of the continents, two conditions must be fulfilled: positive buoyancy and limited deformation within continents (e.g., Doin et al., 1997; Lenardic & Moresi, 1999). We choose a density contrast between continental material and ambient mantle of -100 kg/m^3 that gives a buoyancy ratio (ratio between the density contrast and the thermal density variation) of -0.4. Continents are 100 times more viscous than the ambient mantle and either feature a high yield stress or are entirely exempted from plastic deformation (cf. Table S1). Due to the high rigidity, continental erosion by mantle flow is negligible, and the rafts are stable over billions of years.

We run the simulations using the StagYY code (Tackley, 2008) in spherical annulus geometry (Hernlund & Tackley, 2008) and choose a resolution of $128 \times 1,024$ in the radial and horizontal direction, respectively. Grid refinement close to the top and bottom boundary is employed, resulting in 10- and 15-km-thick cells at the surface and at the core-mantle boundary. To track composition, we use 4×10^7 tracers.

3. Results

3.1. Interaction of Rifting and Global Dynamics

A typical example of rift evolution (scenario A1) within our global convection model is shown in Figure 1, where a suture zone within collided continents is subjected to extension that finally leads to continental rupture and formation of a new ocean basin. Due to the self-consistent nature of our models, rifting events occur when the global buoyancy distribution generates a mantle configuration where the tensional force within the rift exceeds the strength of the suture between the two continents. This takes place when one or more of the following processes occur: (1) A subduction zone adjacent to the continent exerts an extensional force on the continent, (2) large-scale divergent mantle flow emerges beneath the suture dragging the continents away from each other, and (3) a thermal plume impinges at the base of the suture, although this process is less important than the other two in our models. Regardless of the actual processes that contribute to the driving force of rifting, we find a characteristic rift evolution in all our scenarios that is described next.

In the prerift phase, prior to any divergence across the suture, the tensional stress within the continent progressively builds up until it reaches the yield limit within the suture (Figures 1k–1m). Once this happens, divergence gradually starts with initially very slow rifting that continues over several tens of Myrs. At the same time, the stress within the continent remains at maximum level. The accumulated extension across the rift gradually thins the thermal lithosphere, leading to a decrease of rift strength, which in turn causes an increase in divergence velocity. The acceleration of rift velocity during the rift speed-up is mirrored by an abrupt stress drop (Figure 1n). Subsequently, the continents experience breakup at elevated velocity, and a new ocean basin is formed. In model A1, this happens by means of subduction initiation at a surprisingly large distance to the rift. After several tens of Myrs of continental divergence, the global force balance eventually changes such that the continental stress increases again while the continents slow down and drift apart.

The evolution of model A1 is characteristic for many other model scenarios and can best be described by dividing it in several distinct phases (Figure 2). The prerift phase (phase 0) is accompanied by a gradual stress increase at zero extension velocity. Once tensional stresses reach the yield limit, initial rifting (phase 1) gradually starts at very low divergence velocities of less than 1 mm/yr that slowly increase to about 10 mm/yr within

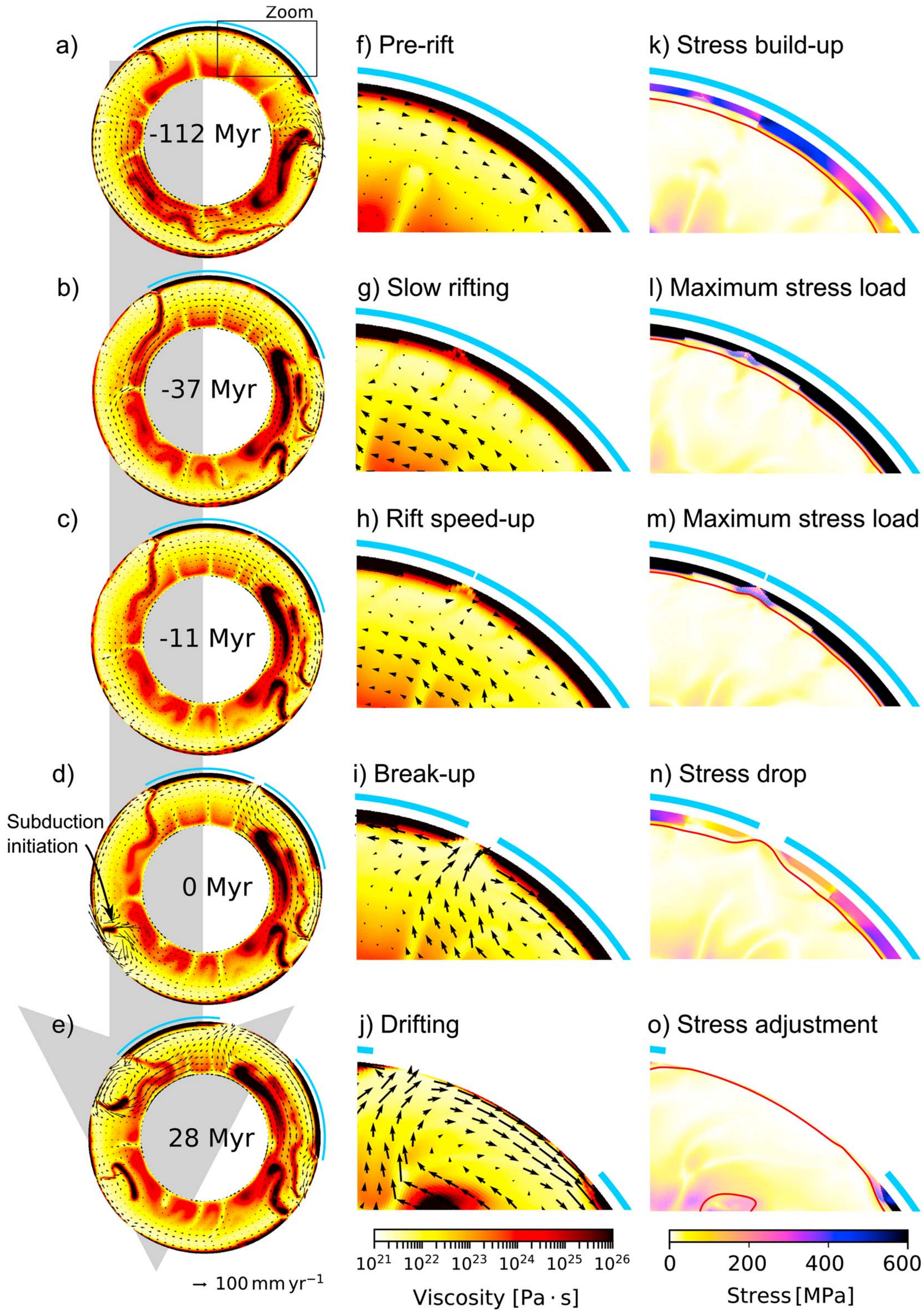

Figure 1. Evolution of reference model A1. (a–e) Mantle viscosity with velocity arrows. Time is increasing downward, and breakup occurs at 0 Myr. (f-j) Close up of viscosity and (k-o) close up of the second invariant of the stress tensor. The 1,200 °C isotherm is shown by red line in the right column. Zoom area is depicted in (a). For visual reference the position of the continents is emphasized in blue. Corresponding rift velocity and stress time series are depicted in Figures 2a and 2b. The full model animation can be found in the supporting information.

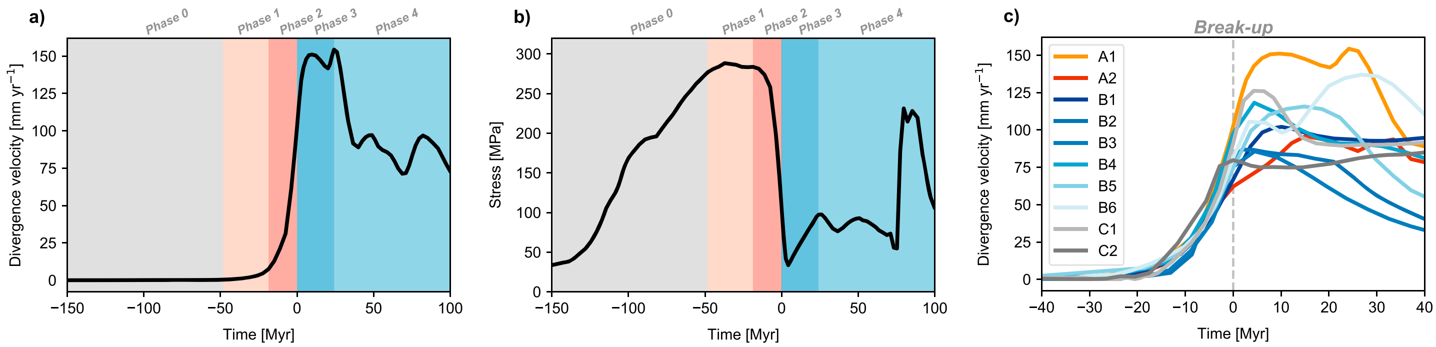

Figure 2. Temporal evolution of divergence velocity and stress. (a) Relative velocity of the continents in model scenario A1 (see Figure 1 for spatiotemporal evolution). (b) Second invariant of the stress tensor in the cratonic continental areas of scenario A1. An average of the stress in the center of the two future continents just below the surface at depth around 10 km is displayed. (c) Rift velocity for all simulated rift cases. Breakup is marked by the dashed vertical line. In all panels, 0 Myr corresponds to breakup time. See supporting information for animations of selected scenarios A1, A2, B1, and C1.

several tens of Myrs. During this phase, the stress load remains at maximum level before it suddenly drops by 80 % within ~10 Myr. Simultaneously, rifting accelerates abruptly by more than 1 order of magnitude (phase 2) and remains at high divergence rates (phase 3) during the onset of seafloor spreading. Within this stage, rift dynamics are governed by a positive feedback loop between extension velocity and rift strength loss, similar to a rope that is stretched until it yields and eventually snaps. Subsequently, the extension velocity drops to intermediate levels of several tens of mm/year while the continental stress increases again (phase 4).

The characteristic history of extension velocity and continental stress is robustly reproduced by alternative scenarios (Table S1). We analyze three groups of models (A, B, and C) differing in lithospheric strength that controls the number and size of the plates (models A and B have strong oceanic lithosphere and larger plates compared to the model group C with weak oceanic lithosphere and smaller plates). Second, the models differ in the strength limit within the continents (high yield strength for model A and no yield limitation for models B and C) that has only minor influence on the dynamics of the system. Cases within one model group (e.g., A1 and A2) represent different rift events for a model with the same parameters but different initial conditions, that is, other random snapshots from the equilibrated part of the evolution. All 10 scenarios depicted in Figure 2c feature the slow initial rift stage followed by abrupt rift acceleration and a high extension rate during the onset of seafloor spreading. The shape of individual velocity histories is very similar during phases 1 and 2; however, it differs during phases 3 and 4. During the postrift phase, seven out of 10 examples exhibit a distinct decrease of postbreakup divergence velocity similar to scenario A1, whereas two examples remain at maximum velocities for more than 40 Myr (B1 and C2), while in another scenario the extension velocity increases even further (A2). The reason for this diversity lies again in the different mantle and plate boundary configurations that exert the dominant control on the kinematic evolution during the postrift phase.

3.2. Comparison with Tectonic Reconstructions

Reconstructions of Pangea breakup not only illustrate the velocity increase during rifting (Brune et al., 2016) suggested by observations from passive margins but also provide quantitative constraints on the evolution of relative plate velocities after breakup through linear magnetic anomalies associated with crust formed by seafloor spreading. Figure 3 shows the plate kinematic history for six successful rifts discussed by Brune et al. (2016), which evolved into sustained seafloor spreading with spreading rate variations recorded across >20 Myr. Decreases in divergence rate within 30 Myr after the speed-up are recorded in the North Atlantic, Central Atlantic, and Australia-Antarctic basins, whereas the divergence rate continues to slowly increase between North America and Greenland. Both the South Atlantic and Iberia-North America rifts reach breakup around the beginning of the Cretaceous Normal Superchron (CNS), a period of >35 Myr during which no isochrons due to magnetic polarity reversals are available to quantitatively constrain changes in divergence rates. Analysis of magnetic anomalies due to variations in magnetic field strength during the CNS (Granot & Dyment, 2015) suggests a progressive increase in South Atlantic divergence rates divergence rates from ~120 to ~80 Ma before dropping in the latest Cretaceous.

Several caveats need to be kept in mind when comparing natural examples to our model results. Changes in divergence rates for these natural examples may be explained by factors not included in the geodynamic models — for example, the collision of Greenland with Ellesmere Island shortly after breakup between

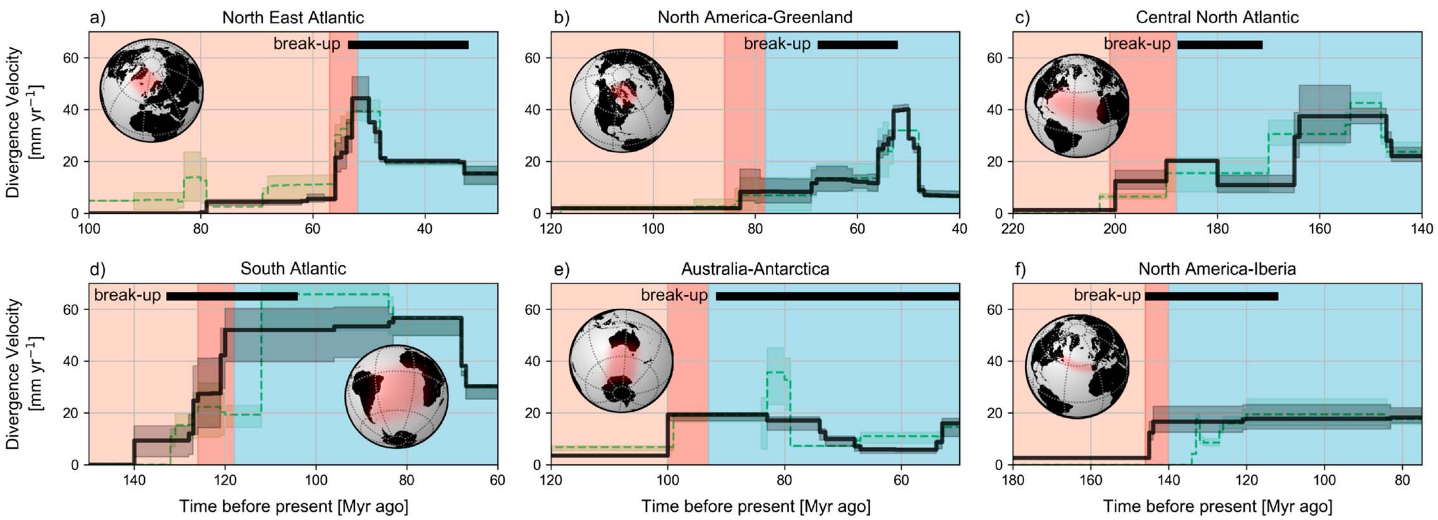

Figure 3. Continent divergence rates from plate tectonic reconstructions (a-f). Black curves illustrate velocity evolution for seed points within the central segment of each rift using reconstruction parameters described in Brune et al. (2016), with bounding gray regions illustrating the variability of rift velocity across the full extent of the rift system. Light green curves show equivalent results using the alternative reconstructions collated by Seton et al. (2012). The black bar at the top of each panel defines the timespan of diachronous breakup (see Brune et al., 2016, for detail).

Greenland and Eurasia may explain the pronounced slow-down in North Atlantic divergence rates (Gaina et al., 2009). The relationship between the timing of rift velocity increase and breakup is likely to differ between our 2-D models and natural examples (where breakup is defined by the onset of seafloor spreading). This is due to the fact that (1) progressive unzipping of continents on a spherical Earth persisting for 25 Myr (e.g., South Atlantic) or more (e.g., Australia-Antarctica) means that breakup for natural examples is prolonged and complex compared to the relatively discrete breakup in the 2-D models and (2), in nature, continental extension or mantle exhumation may continue for significant periods beyond the time of rift-strength loss resulting in a delay between rift velocity increase and breakup (Figure 3), whereas this process is not captured in our 2-D model cases (and we instead define breakup for the model cases as the moment of lithospheric rupture). The timing of velocity changes in Figure 3 is dependent on the timing of interpreted magnetic isochrons, and the relatively coarse sampling of these isochrons in many basins (~5–10 Myr and much greater in the CNS) allows for greater variability in initial spreading rates than captured by reconstructions (Lundin et al., 2018).

4. Discussion and Conclusion

It has been previously suggested that continental rifting typically involves a slow-fast kinematic evolution due to the interaction of internal rift weakening with far-field plate driving forces (Brune et al., 2016). Here we reproduce the previous findings concerning the rift stage but also gain new insight concerning the postrift evolution. Phase 1 corresponds to the initial rift stage of slow rifting where the extensional stress level is controlled by the lithospheric yield strength. Phase 2 comprises the rift acceleration period and is marked by an abrupt increase of extension rate and a simultaneous stress drop that corresponds to rift strength loss due to necking of the lithosphere. Note that the coeval change in velocity and stress can only be addressed in models without lateral boundaries, that is, without prescribing either a boundary velocity or a boundary force. The fact that we reproduce previously suggested rift kinematics with a more general model setup therefore lends further robustness to these findings. Continental breakup takes place at the beginning of phase 3, and hence, extension velocity during phase 3 is no longer controlled by rift strength but by the global force balance. The different amplitudes of the presented models therefore relate to the diverse mantle and plate boundary configurations in the individual models. Maximum postrift velocities last from 5 Myr to more than 40 Myr depending on the longevity of mantle structure and plate boundary configuration. Many models display a distinct phase 4 where divergence velocities decrease gradually. This can be understood when considering that only certain combinations of mantle drag and plume impingement beneath the continent or subduction geometries adjacent to the continent generate sufficient tensional stress to overcome the lithospheric strength at the continental suture. During the postrift phase, these configurations typically continue driving the plates in the same directions at an elevated speed; however, the velocity of the plates is prone to decrease once the large-scale configuration eventually changes.

Since the surface area of the Earth is constant, every change in rift kinematics has to be compensated by changes in relative motion at other plate boundaries. The abrupt velocity increase during phase 2 therefore induces enhanced convergence in many model scenarios. This model outcome predicts enhanced subduction velocities, for instance for North America and the Farallon plate during Central Atlantic rifting in the Early Jurassic or closure of back-arc basins as inferred in the proto-Andean ranges of South America during South Atlantic opening (Maloney et al., 2013). Interestingly, compensation of rift acceleration does not necessarily take place adjacent to the two plates involved in the rift event but often occurs in locations far from the model continents. Scenarios A1, B1, and C1, for instance, exhibit subduction initiation at large distance from the continents, contemporaneous to the rift acceleration (see supporting information animations). A similar effect takes place in scenario A2, where the convergence rate at distant subduction zones rapidly increases during rift phase 3. To quantify the link between rifting and subduction initiation in a statistical way, we analyzed the strong lithosphere scenarios (model groups A and B) where the number of subduction zones is best representative of Earth. Of these eight rift scenarios, five events feature subduction initiation within 15 Myr before breakup. Additionally, these models exhibit subduction initiation on average ~2.4 times per 100 Myr, independent of rift occurrence. Hence, the probability for subduction initiation during 15 Myr is 0.63 during a rift event, but almost two times lower, namely, 0.36, without rifting. Due to the low number of rift cases the rift-related probability includes a degree of uncertainty; nevertheless, the impact of rifting on subduction initiation appears to be statistically significant. We speculate that existing subduction zones do not actually constitute weak spots that easily accommodate more convergence. Instead, the cold and rigid subducting slabs (see Figure 1) connect the high-viscosity lithosphere to the high-viscosity lower mantle. Due to this coupling, rift-related displacements of the lithosphere cannot always change the convergence rate at an existing subduction zone and instead may induce subduction initiation at another location. However, subduction inception very far from the continents might be biased due to the 2D- character of our simulations. In 3-D geometry, there may be more ways to accommodate the increased divergence, as mantle flow and plate motions can occur in orthogonal direction to the 2-D plane and hence change the location of subduction initiation.

These results point to a causal relationship between rift acceleration and global plate reorganization. Global plate tectonic reconstructions reveal abrupt, widespread changes in plate motion and boundary configurations, notably at ~50 and ~100 Myr ago (Matthews et al., 2012; Whittaker et al., 2007), which have variably been attributed to ridge subduction, plume-push forces, and continent-continent collision. Eocene plate motion change is contemporaneous with the initiation of major new intraoceanic subduction zones across a wide region of the western Pacific presently represented by the Izu-Bonin-Mariana and Tonga-Kermadec systems (Gurnis et al., 2004). Current hypotheses suggest a role for both local lithospheric buoyancy variations and plate-scale compressional forces (Arculus et al., 2015; Sutherland et al., 2017), yet the ultimate trigger for these new plate boundaries to form by either mechanism remains unclear. Our model results allow us to propose the far-field effect of rift acceleration and breakup in the North Atlantic and Eurasia Basin (~55 Myr ago) as an alternative, plausible catalyst for distal, almost contemporaneous changes in plate boundary configuration and force balance. The details of earlier subduction initiations are less clear, but mid-Cretaceous subduction initiation within the Tethys ocean (Guilmette et al., 2018; Maffione et al., 2017) could be connected to increases in rift velocity within the South Atlantic and between Australia and Antarctica.

When interpreting the numerical results one should keep in mind that there are certain model limitations. Several lithospheric weakening mechanisms are not accounted for such as strain softening, intrusion-related heating, shear heating, and structural softening (Duretz et al., 2015, 2016; Huismans et al., 2005). Lithospheric deformation of plate boundaries on Earth has a memory of previous yielding, but our rheological description neglects any deformation history and reflects instantaneous stress distribution. Therefore, the change in extension rate in our convection models must be seen as a lower bound to the rift acceleration in nature. In the model design, we made a number of assumptions that might influence the style of rifting. Importantly, we fix the internal heating rate so that plumes in the models are weak and do not add much driving force for rifting. Decreasing the internal heating and thus increasing the strength of the plumes might result in plume-induced rifting (Koptev et al., 2015). Also, rifting might be facilitated by having weak continental margins (Rolf et al., 2014) while here we assume them to have the same rigidity as the continental interior. Timing of rifting is related to the mantle structures such as size of convective cells (Rolf et al., 2014) that are probably larger here compared to the Earth due to the lower convective vigor, which lead us to employ a transit time framework to scale the results and compare them to observations. Employing standard scaling using the diffusive time would result in ∼4 times lower rift velocities, while simultaneously leading to ∼4 times longer durations of each rift phase. Ideally, both scalings should result in the same average Earth-like velocities, given that we use "realistic" Earth parameters representing our planet including a suitable rheological law. Note that using a different scaling formulation would affect the absolute values in Figure 2 but does not change our overall conclusions.

A major advantage of the presented models over previous Cartesian box rift models with velocity or force boundary conditions is that the spherical annulus geometry does not require lateral boundary conditions to be specified, simply because there are no lateral boundaries. While it is not computationally feasible for mantle convection models to employ high-resolution and complex rheology as is commonly employed in lithospheric-scale setups, the new results can nevertheless be used to infer which type of boundary condition in Cartesian box simulations is most realistic for a given setting. (1) If the modeling setup focuses on lithospheric-scale weakening processes and the associated stress evolution during phase 1, we find that constant force boundary conditions are most appropriate, because the stress during this phase is almost constant (Figure 2b). (2) If however the setup addresses late rift stages or the transition from rifting to seafloor spreading, we recommend constant velocity boundary conditions, since the divergence velocity does not change much during phase 3. The same is true when investigating the evolution of a small basin where there is no feedback between rift dynamics and large-scale plate motions. Note that during phase 2, the global force balance interacts with the rift strength loss and neither local nor global processes can be neglected.

In summary, we conclude that geodynamic and plate tectonic modeling suggests a multiphase velocity behavior during continental rifting that is controlled by the interaction of rift dynamics with far-field forces. In our models, rifting involves a characteristic speed-up and often a later slow down of plate divergence, comparable with natural examples. These changes in plate motion are expected to be mirrored elsewhere either by enhanced convergence rates at an existing trench or through initiation of a new subduction zone.

Acknowledgments
The support for this research has been provided by the European Union's Horizon 2020 Research and Innovation Program under the ERC grant agreement 617588 and the Marie Skłodowska Curie grant agreement 753755, the German Academic Exchange Service (DAAD) project 57319603, the Helmholtz Association through the Young Investigators Group CRYSTALS (VH-NG-1132), and the Australian Research Council Grants IH130200012 and DP180102280. Simulations were performed on the AUGURY supercomputer at P2CHPD Lyon. The StagPy library was used in this study to process StagYY output data (`https://github.com/StagPython/StagPy`). The authors thank N. Coltice for his comments on this work, P. Tackley for providing the StagYY code, and T. Rolf and S. Buiter for constructive and motivating reviews that helped to improve the manuscript. Data used to run the StagYY are available in the supporting information.

References

Ammann, N., Liao, J., Gerya, T., & Ball, P. (2017). Oblique continental rifting and long transform fault formation based on 3D thermomechanical numerical modeling. *Tectonophysics*, *746*, 106–120. https://doi.org/10.1016/j.tecto.2017.08.015

Arculus, R. J., Ishizuka, O., Bogus, K. A., Gurnis, M., Hickey-Vargas, R., Aljahdali, M. H., et al. (2015). A record of spontaneous subduction initiation in the Izu-Bonin-Mariana arc. *Nature Geoscience*, *8*, 728–733.

Armitage, J. J., Petersen, K. D., & Pérez-Gussinyé, M. (2018). The role of crustal strength in controlling magmatism and melt chemistry during rifting and breakup. *Geochemistry, Geophysics, Geosystems*, *19*, 534–550. https://doi.org/10.1002/2017GC007326

Brune, S. (2016). Rifts and rifted margins: A review of geodynamic processes and natural hazards. *Plate Boundaries and Natural Hazards*, *219*, 11–37.

Brune, S. (2018). Forces within continental and oceanic rifts: Numerical modeling elucidates the impact of asthenospheric flow on surface stress. *Geology*, *46*, 191.

Brune, S., Heine, C., Clift, P. D., & Pérez-Gussinyé, M. (2017). Rifted margin architecture and crustal rheology: Reviewing iberia-newfoundland, central South Atlantic, and South China sea. *Marine and Petroleum Geology*, *79*, 257–281.

Brune, S., Heine, C., Pérez-Gussinyé, M., & Sobolev, S. V. (2014). Rift migration explains continental margin asymmetry and crustal hyper-extension. *Nature Communications*, *5*, 4014.

Brune, S., Popov, A. A., & Sobolev, S. V. (2012). Modeling suggests that oblique extension facilitates rifting and continental break-up. *Journal of Geophysical Research*, *117*, B08402. https://doi.org/10.1029/2011JB008860

Brune, S., Popov, A. A., & Sobolev, S. V. (2013). Quantifying the thermo-mechanical impact of plume arrival on continental break-up. *Tectonophysics*, *604*, 51–59.

Brune, S., Williams, S. E., Butterworth, N. P., & Müller, R. D. (2016). Abrupt plate accelerations shape rifted continental margins. *Nature*, *536*, 201–204.

Buck, W. (2015). Dynamic processes in extensional and compressional settings: The dynamics of continental breakup and extension (2nd ed.). In G. Schubert (Ed.), *Treatise on Geophysics* (pp. 325–379). Oxford: Elsevier.

Coltice, N., Gérault, M., & Ulvrová, M. (2017). A mantle convection perspective on global tectonics. *Earth-Science Reviews*, *165*, 120–150.

Coltice, N., Rolf, T., Tackley, P. J., & Labrosse, S. (2012). Dynamic causes of the relation between area and age of the ocean floor. *Science*, *336*, 335–338.

Crameri, F., Tackley, P. J., Meilick, I., Gerya, T. V., & Kaus, B. J. P. (2012). A free plate surface and weak oceanic crust produce single-sided subduction on earth. *Geophysical Research Letters*, *39*, L03306. https://doi.org/10.1029/2011GL050046

Davis, J. K., & Lavier, L. L. (2017). Influences on the development of volcanic and magma-poor morphologies during passive continental rifting. *Geosphere*, *13*, 1524–1540.

Doin, M. P., Fleitout, L., & Christensen, U. (1997). Mantle convection and stability of depleted and undepleted continental lithosphere. *Journal of Geophysical Research*, *102*, 2771–2787.

Duretz, T., Petri, B., Mohn, G., Schmalholz, S. M., & Schenker, F. L. (2016). The importance of structural softening for the evolution and architecture of passive margins. *Scientific Reports*, *6*, 38704.

Duretz, T., Schmalholz, S. M., & Podladchikov, Y. Y. (2015). Shear heating-induced strain localization across the scales. *Philosophical Magazine*, *0*, 1–16.

Forsyth, D., & Uyeda, S. (1975). On the relative importance of the driving forces of plate motion. *Geophysical Journal International*, *43*, 163–200.

Gaina, C., Gernigon, L., & Ball, P. (2009). Palaeocene—Recent plate boundaries in the NE Atlantic and the formation of the Jan Mayen microcontinent. *Journal of the Geological Society*, *166*, 601–616.

Gerya, T. V., Connolly, J. A., & Yuen, D. A. (2008). Why is terrestrial subduction one-sided? *Geology*, *36*, 43–46.

Granot, R., & Dyment, J. (2015). The cretaceous opening of the South Atlantic Ocean. *Earth and Planetary Science Letters*, *414*, 156–163.

Guilmette, C., Smit, M. A., van Hinsbergen, D. J. J., Gürer, D., Corfu, F., Charette, B., et al. (2018). Forced subduction initiation recorded in the sole and crust of the Semail ophiolite of Oman. *Nature Geoscience*, *11*, 688–695.

Gurnis, M., Hall, C., & Lavier, L. (2004). Evolving force balance during incipient subduction. *Geochemistry, Geophysics, Geosystems*, *5*, Q07001. https://doi.org/10.1029/2003GC000681

Heine, C., & Brune, S. (2014). Oblique rifting of the equatorial atlantic: Why there is no saharan atlantic ocean. *Geology*, *42*, 211–214.

Heine, C., Zoethout, J., & Müller, R. (2013). Kinematics of the South Atlantic rift. *Solid Earth*, *4*, 215–253.

Hernlund, J. W., & Tackley, P. J. (2008). Modeling mantle convection in the spherical annulus. *Physics of the Earth and Planetary Interiors*, *171*, 48–54.

Huismans, R. S., & Beaumont, C. (2003). Symmetric and asymmetric lithospheric extension: Relative effects of frictional-plastic and viscous strain softening. *Journal of Geophysical Research*, *108*(B10), 2496. https://doi.org/10.1029/2002JB002026

Huismans, R. S., Buiter, S. J. H., & Beaumont, C. (2005). Effect of plastic-viscous layering and strain softening on mode selection during lithospheric extension. *Journal of Geophysical Research*, *110*, B02406. https://doi.org/10.1029/2004JB003114

Jaupart, C., Labrosse, S., Lucazeau, F., & Mareschal, J. (2015). 7.06 - Temperature, Heat, and Energy in the Mantle of the Earth, (2nd ed.). In G. Schubert (Ed.), *Treatise on Geophysics (Second Edition)* (pp. 223–270). Oxford: Elsevier.

Kneller, E. A., Johnson, C. A., Karner, G. D., Einhorn, J., & Queffelec, T. A. (2012). Inverse methods for modeling non-rigid plate kinematics: Application to mesozoic plate reconstructions of the central atlantic. *Computers & Geosciences*, *49*, 217–230.

Koptev, A., Calais, E., Burov, E., Leroy, S., & Gerya, T. (2015). Dual continental rift systems generated by plume–lithosphere interaction. *Nature Geoscience*, *8*, 388–392.

Lenardic, A., & Moresi, L. N. (1999). Some thoughts on the stability of cratonic lithosphere: Effects of buoyancy and viscosity. *Journal of Geophysical Research*, *104*, 12,747–12,758.

Lundin, E. R., Doré, A. G., & Redfield, T. F. (2018). Magmatism and extension rates at rifted margins. *Petroleum Geoscience*, *24*, 379–392. https://doi.org/10.1144/petgeo2016-158

Maffione, M., van Hinsbergen, D. J., de Gelder, G. I., van der Goes, F. C., & Morris, A. (2017). Kinematics of late cretaceous subduction initiation in the neo-tethys ocean reconstructed from ophiolites of Turkey, Cyprus, and Syria. *Journal of Geophysical Research: Solid Earth*, *122*, 3953–3976. https://doi.org/10.1002/2016JB013821

Maloney, K. T., Clarke, G. L., Klepeis, K. A., & Quevedo, L. (2013). The Late Jurassic to present evolution of the Andean margin: Drivers and the geological record. *Tectonics*, *32*, 1049–1065. https://doi.org/10.1002/tect.20067

Matthews, K. J., Seton, M., & Müller, R. D. (2012). A global-scale plate reorganization event at 105–100 Ma. *Earth and Planetary Science Letters*, *355-356*, 283–298.

McQuarrie, N., & Wernicke, B. P. (2005). An animated tectonic reconstruction of southwestern North America since 36 Ma. *Geosphere*, *1*, 147–172.

Mondy, L. S., Rey, P. F., Duclaux, G., & Moresi, L. (2017). The role of asthenospheric flow during rift propagation and breakup. *Geology*, *46*, 103–106.

Moresi, L., & Solomatov, V. (1998). Mantle convection with a brittle lithosphere: Thoughts on the global tectonic styles of the Earth and Venus. *Geophysical Journal International*, *133*, 669–682.

Müller, R. D., Seton, M., Zahirovic, S., Williams, S. E., Matthews, K. J., Wright, N. M., et al. (2016). Ocean basin evolution and global-scale plate reorganization events since Pangea breakup. *Annual Review of Earth and Planetary Sciences*, *44*, 107–138.

Naliboff, J., & Buiter, S. J. H. (2015). Rift reactivation and migration during multiphase extension. *Earth and Planetary Science Letters*, *421*, 58–67.

Pérez-Gussinyé, M., Morgan, J. P., Reston, T. J., & Ranero, C. R. (2006). The rift to drift transition at non-volcanic margins: Insights from numerical modelling. *Earth and Planetary Science Letters*, *244*, 458–473.

Rolf, T., Capitanio, F., & Tackley, P. (2017). Constraints on mantle viscosity structure from continental drift histories in spherical mantle convection models. *Tectonophysics*, *746*, 339–351. https://doi.org/10.1016/j.tecto.2017.04.031

Rolf, T., Coltice, N., & Tackley, P. (2014). Statistical cyclicity of the supercontinent cycle. *Geophysical Research Letters*, *41*, 2351–2358. https://doi.org/10.1002/2014GL059595

Rolf, T., & Tackley, P. (2011). Focussing of stress by continents in 3D spherical mantle convection with self-consistent plate tectonics. *Geophysical Research Letters*, *38*, L18301. https://doi.org/10.1029/2011GL048677

Salerno, V. M., Capitanio, F. A., Farrington, R. J., & Riel, N. (2016). The role of long-term rifting history on modes of continental lithosphere extension. *Journal of Geophysical Research: Solid Earth*, *121*, 8917–8940. https://doi.org/10.1002/2016JB013005

Seton, M., Mller, R., Zahirovic, S., Gaina, C., Torsvik, T., Shephard, G., et al. (2012). Global continental and ocean basin reconstructions since 200 Ma. *Earth-Science Reviews*, *113*, 212–270.

Sutherland, R., Collot, J., Bache, F., Henrys, S., Barker, D., Browne, G., et al. (2017). Widespread compression associated with Eocene Tonga-Kermadec subduction initiation. *Geology*, *45*, 355–358.

Tackley, P. J. (2000a). *The quest for self-consistent generation of plate tectonics in mantle convection models, Geophysical Monograph Series* (Vol. 121, pp. 47–72). Washington, DC: American Geophysical Union.

Tackley, P. J. (2000b). Self-consistent generation of tectonic plates in time-dependent, three-dimensional mantle convection simulations 1. Pseudoplastic yielding. *Geochemistry, Geophysics, Geosystems*, *1*. https://doi.org/10.1029/2000GC000036

Tackley, P. J. (2008). Modelling compressible mantle convection with large viscosity contrasts in a three-dimensional spherical shell using the yin-yang grid. *Physics of the Earth and Planetary Interiors*, *171*, 7–18.

Tackley, P. J., & King, S. D. (2003). Testing the tracer ratio method for modeling active compositional fields in mantle convection simulations. *Geochemistry, Geophysics, Geosystems*, *4*(4), 8302. https://doi.org/10.1029/2001GC000214

Tagawa, M., Nakakuki, T., Kameyama, M., & Tajima, F. (2007). The role of history-dependent rheology in plate boundary lubrication for generating one-sided subduction. *Pure and Applied Geophysics*, *164*, 879–907.

Takeshita, T., & Yamaji, A. (1990). Acceleration of continental rifting due to a thermomechanical instability. *Tectonophysics*, *181*, 307–320.

Tetreault, J., & Buiter, S. (2018). The influence of extension rate and crustal rheology on the evolution of passive margins from rifting to break-up. *Tectonophysics*, *746*, 155–172. Understanding geological processes through modelling—A Memorial volume honouring Evgenii Burov.

Turcotte, D. L., & Schubert, G. (2002). *Geodynamics* (2nd ed.). New York: Cambridge University Press.

Whittaker, J. M., Müller, R. D., Leitchenkov, G., Stagg, H., Sdrolias, M., Gaina, C., & Goncharov, A. (2007). Major Australian-Antarctic plate reorganization at Hawaiian-Emperor bend time. *Science*, *318*, 83–86.

Ziegler, P. A., & Cloetingh, S. (2004). Dynamic processes controlling evolution of rifted basins. *Earth-Science Reviews*, *64*, 1–50.